

# Experimental Investigation and Numerical Analysis of Flow Past Airfoils with Spoilers and High Lift Devices

Natalie Souckova, Milan Matejka  
*Department of Fluid Dynamics and Thermodynamics, FME, Czech Technical University in Prague,  
Prague, CZ 166 07, Czech Republic  
Natalie.Souckova@fs.cvut.cz*

Lukas Popelka  
*Institute of Thermomechanics, Academy of Sciences of the Czech Republic,  
Prague, CZ 182 00, Czech Republic  
popelka@it.cas.cz*

## Abstract

The paper focuses on airfoils with spoilers and high lift devices. The investigation was carried out using experimental and numerical methods. Results of two methods of visualization (Particle Image Velocimetry, Smoke wire) for three types of airfoils (two with different spoilers and one with a split flap) were extended by pressure distribution measurement for one airfoil. The measurements were taken in open and closed circuit wind tunnels. Pressure distribution, velocity profile and images of flow in the airfoil vicinity were evaluated from numerical computations. The obtained data was prepared for mutual comparison and results were discussed.

## Introduction

The role of high lift devices and spoilers or air brakes is considerable and there exist a number of reports related to this topic. Nevertheless, the majority of them target only the different kinds of flaps. The most comprehensive experimental work concerning air brakes originates from Institut für Aero - und Gasdynamik der Universität Stuttgart<sup>1</sup>. The other important work is focused on different spoiler geometries located in a rear part of an airfoil and using spoilers and deflected Fowler flap together<sup>2</sup>. However, the published lift, drag and moment characteristics of airfoils with spoiler flaps and dive brakes in different positions are not sufficient for thorough understanding of the flow field. This study adds further information to that knowledge.

## Experiment

The experimental part of the investigation consisted of three types of measurements intended for comparison with numerical analysis. All experiments were conducted in the general purpose wind tunnels of the Fluid Dynamics Laboratory Division of FME, CTU in Prague<sup>3,4</sup>.

### PIV – Particle Image Velocimetry

The measurement was carried out in a closed circuit wind tunnel with an open test section of cross-section 750 mm by 550 mm at Reynolds number  $Re = 3.3 \cdot 10^5$ , at two angles of attack  $\alpha = 0$  and 6 degs. and with turbulence intensity of  $Tu = 3.8\%$ . The models used had chords of 300 mm and spans of 400 mm. The airfoils used included an FX66-17AII-182 with dive brake (extending type, also referred as SH type), an NACA 23012 with spoiler flap (DFS type) and an MS (1)-0313<sup>5</sup> with split flap. The geometry of drag and lift control

devices was taken from particular sailplane applications (Standard Cirrus and LK425 Sohaj 3) and tow aircraft. Models were located in the open test section by a fixture with annular end plates of transparent plexiglass. Spoilers and split flap were fixed between the plates. The non-contact laser method was used to visualize the flowfield in the small regions of the given airfoils as depicted in Figs. 1 - 3.

### Smoke – wire visualization

The traditional smoke-wire technique was used for supplemental information about the flow in sections of the leading and trailing edges on the NACA 23012 airfoil with a spoiler. The main objective of this experiment was the verification of the numerical results, especially the position of the stagnation point on the leading edge, and to explore the existence of vortex structures in the vicinity of the trailing edge. Measurements were obtained at zero angle of attack and, to achieve reasonable image quality, at the small velocity of approximately 2 m/s. The smoke for the visualization was generated by two coiled wires heated by electrical current and covered with glycerine. The location of the wires in the input part of the test section made it possible to set the model at the same location at which the PIV measurements were made.

### Pressure distribution measurement

Pressure distribution measurements were performed for the FX66-17AII-182 airfoil with and without the dive brake deployed. These measurements were made in an open circuit wind tunnel having a closed 1200mm by 400mm test section. The Reynolds number was the same as for the PIV measurements and turbulence intensity was  $Tu = 1.2\%$ . The angle of attack was set over the range of -2 to 12.5 degs. The model had a chord of 400mm, a span of 400mm, and was equipped with a single row of pressure orifices located in the

middle of the span on the upper and lower surfaces. It was mounted vertically between the upper and lower sides of the test section, as shown in Fig. 4, thereby achieving two-dimensional flow. Lift coefficients were calculated from the surface pressure distribution and standard wind-tunnel correction were applied.

### Numerical Analysis

The same geometry used for the wind-tunnel experiments was employed for the Computational Fluid Dynamics (CFD) analysis of the NACA 23012 airfoil with the deployed spoiler. Likewise, CFD was applied to the FX66-17AII-182 airfoil having a chord of 300mm with dive brake, as well as to the 400 mm chord with and without a deployed dive brake.

The computational area is composed of two areas in shape “C”, where one of them is near the profile and the second area has borders at a certain distance enabling boundary conditions for free stream flow (Fig. 5). A combination of structured mesh near the airfoil and unstructured mesh, of triangular shape elements away from it, was applied (Fig. 6). Computational areas have 158,624 cells for the NACA 23012 airfoil, 138,123 cells for the FX66-17AII-182 airfoil having the 300 mm chord, and 143,885 for the same airfoil having a 400 mm chord. Steady, two-dimensional incompressible viscous flow was solved. The commercial code Fluent version 6.2 enabled only an assumption of a fully turbulent free stream flow and in combination with insignificant molecular viscosity the  $k-\epsilon$  model to assess turbulent flow was applied. This numerical model is well suited for computational efficiency, robustness, relatively good accuracy and little computational time. With respect to mesh used, a second order upwind discretization scheme was employed. Input parameters are summarized in Table. 1.

### Results

The results of the PIV experiment, namely fields of velocity magnitude and velocity vectors, shown in Fig. 7 and 8, depict the flow separation present on both types of spoilers, back flow, vortices, and wide wake. Time-averaged velocity profiles conform to the generally accepted flow patterns; however, instantaneous velocity fields show that such a flowfield was never realized – vortex shedding dominated the area past the spoilers.

The split flap caused the lift to increase by influencing the camber change of the airfoil as is known from theory<sup>6</sup>. The measurements shown in Fig. 9 (left) indicate a wide wake which causes a drag increase in addition to the instantaneous image of the flow behind the flap, which shows vortices shedding.

The numerical analysis provides information on the velocity field around the airfoils in Figs. 10 and 11, showing stagnation points on the leading edges, flow separation on the front upper side of the spoiler and a subsequent area of separated flow extending to the trailing edge. Also, there is

a negative lift force generated at zero angle of attack which corresponds to results reported in Ref. 1. Comparison of the lift-curve slopes for the airfoil with and without spoiler, shown in Fig. 12, confirms this behaviour. The determination of the drag force was not possible from numerical analysis, as the steady-type computation used are unable to predict the unsteady flow past the spoiler, nor was it possible experimentally due to equipment limitations, such as the general purpose wind tunnel. Images of velocity fields as well as velocity profiles in specific locations, Figs. 13, 14, reflect the agreement between experimental and numerical results. Both methods revealed significant flow separation that was responsible for a considerable drag increase.

The position of stagnation point on leading edge of the NACA 23012 airfoil was verified by smoke-wire visualization, as shown in Figs. 15 and 16.

### Conclusions

The 2D experimental investigation presented here provides considerable helpful information and physical insight into split flap and spoilers effects on flow including flowfield changes, vorticity production and lift changes. Although all measurements were carried out at quite low Reynolds number due to the available equipments, the results focused on lift slope differences rather than absolute values. The physical principles are not violated by these limitations, thus the results are still useful. This conclusion is supported by lift slopes results measured in Institut für Aero - und Gasdynamik der Universität Stuttgart<sup>1</sup>.

Nevertheless, much more is still required, especially to aid in the design of lift and drag control devices. Additional information about the forces produced by lift and drag devices is needed, as well as information regarding the effects of these devices on the other parts of the aircraft. The same problems are encountered in 2D steady state numerical simulations. And, moreover, the fully turbulent flow expected does not correspond to reality. Despite this, the velocity distribution conformed with the experiment and, thus, the calculations provide a simple and fast tool not only for fundamental physical insight, but also a means for optimization of the flow control devices. But, using a more suitable code that includes at least a laminar-turbulent flow transition is necessary for future investigations.

It is possible to obtain additional information with three-dimensional measurements and numerical computations. The numerical computations would be more complete, due to the possibility of obtaining information about flow near the airfoil as well as further downstream. On the other hand, there is a problem with the accuracy of the solution. It is essential to compute unsteady flow with a time step corresponding to the frequency of the vortex shedding on the spoiler to get information about the forces. In addition, it is necessary to perform a specialized measurement to determine the forces. Therefore, future work should combine both experimental and computational approaches.

## Acknowledgments

The research was supported by the Ministry of Education, Youth and Sports of The Czech Republic, within project No. 1M06031, by the Grant Agency of the Czech Republic, within project No. 101/08/1112 and Grant Agency of the Academy of Sciences of the CR, project No. IAA2076403.

## References

<sup>1</sup>Althaus, D., Wortmann, F.X., *Stuttgarter Profilkatalog I*, 1st ed., Vieweg & Sohn Verlagsgesellschaft, Braunschweig, 1981, 319 p.

<sup>2</sup>Wentz, W.H., Volk, C.G., "Reflection-plane Tests of Spoilers on an Advanced Technology Wing with a Large Fowler Flap," NASA report NASA CR - 2696, 1976, 88 p. Available at WWW: <http://ntrs.nasa.gov/search.jsp>

<sup>3</sup>Antos, P., Sulitka, M., "Update of Aerodynamic Closed-Circuit Wind Tunnel of the Fluid Dynamics Department CTU in Prague" XVIII<sup>th</sup> International Research Conference on Application of Experimental and Numerical Methods in Fluid Dynamics, Žilina University, Žilina, 2002, pp. 126-131.

<sup>4</sup>Popelka, L., "Aerodynamic Wind Tunnel 1200x400mm," Research report VZ 203/06, CTU, Faculty of Mechanical Engineering, Prague, 2006, 12 p.

<sup>5</sup>McGhee, R.J., Beasley, W.D., "Low-speed aerodynamic characteristic of a 13-percent-thick medium-speed airfoil section designed for general aviation applications" NASA TP-1498, 1979

<sup>6</sup>Schlichting, H., Truckenbrodt, E., Ramm, H.J., *Aerodynamics of the Airplane*, Osborne-McGraw-Hill, USA, 1979, 541 p.

**Table 1**

Input parameters of the numerical solutions

( $v$  – free stream velocity,  $Re$  - Reynolds number,  $Tu$  – turbulence intensity,  $L_k$  - length scale of turbulence,  $\alpha$  - angle of attack)

Airfoils	$v$ [m/s]	$Re$ [-]	$Tu$ [%]	$L_k$ [m]	$\alpha$ [deg]
NACA 23012	16	$3.33 \cdot 10^5$	3.78	0.0038	0
FX 66-17AII-182 $c = 300$ mm	16	$3.33 \cdot 10^5$	3.78	0.0038	0
FX 66-17AII-182 $c = 400$ mm	12.8	$3.33 \cdot 10^5$	1.2	0.0012	0

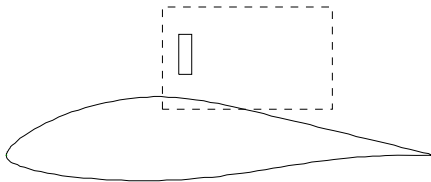


**Figure 1** Contour of FX66-17AII-182 airfoil with area of interest in the dashed box.

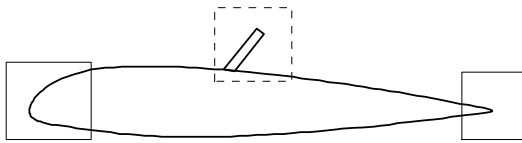


**Figure 2** Contour of NACA 23012 airfoil with areas of interest in the dashed and solid boxes.

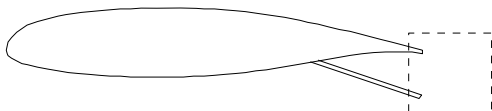


**Figure 3** Contour of MS (1)-0313 airfoil with area of interest in the dashed box.



**Figure 4** Model of airfoil FX66-17AII-182 in test section of open circuit wind tunnel with closed test section.

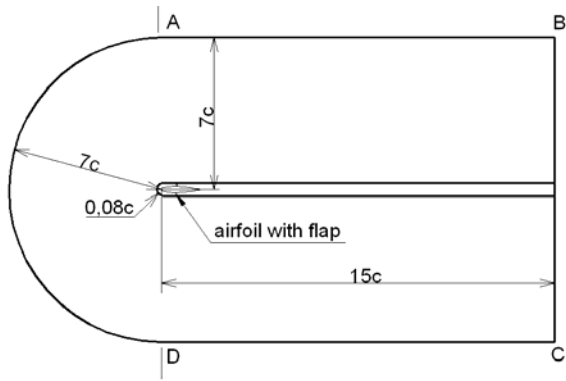


**Figure 5** Computational area ( $c$  = chord length).

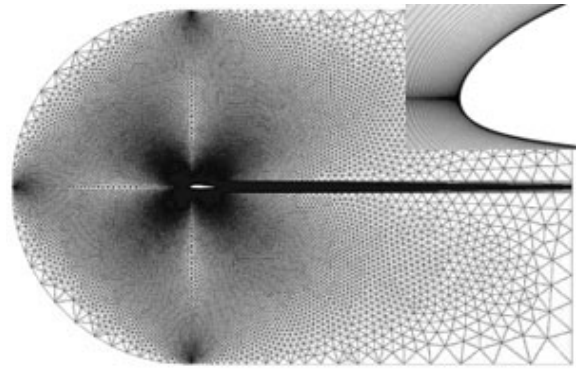


**Figure 6** Computational mesh.

**Editors comment:** the gray shades in the figures that follow are defined in the color images at [journals.sfu.ca/ts/](http://journals.sfu.ca/ts/).

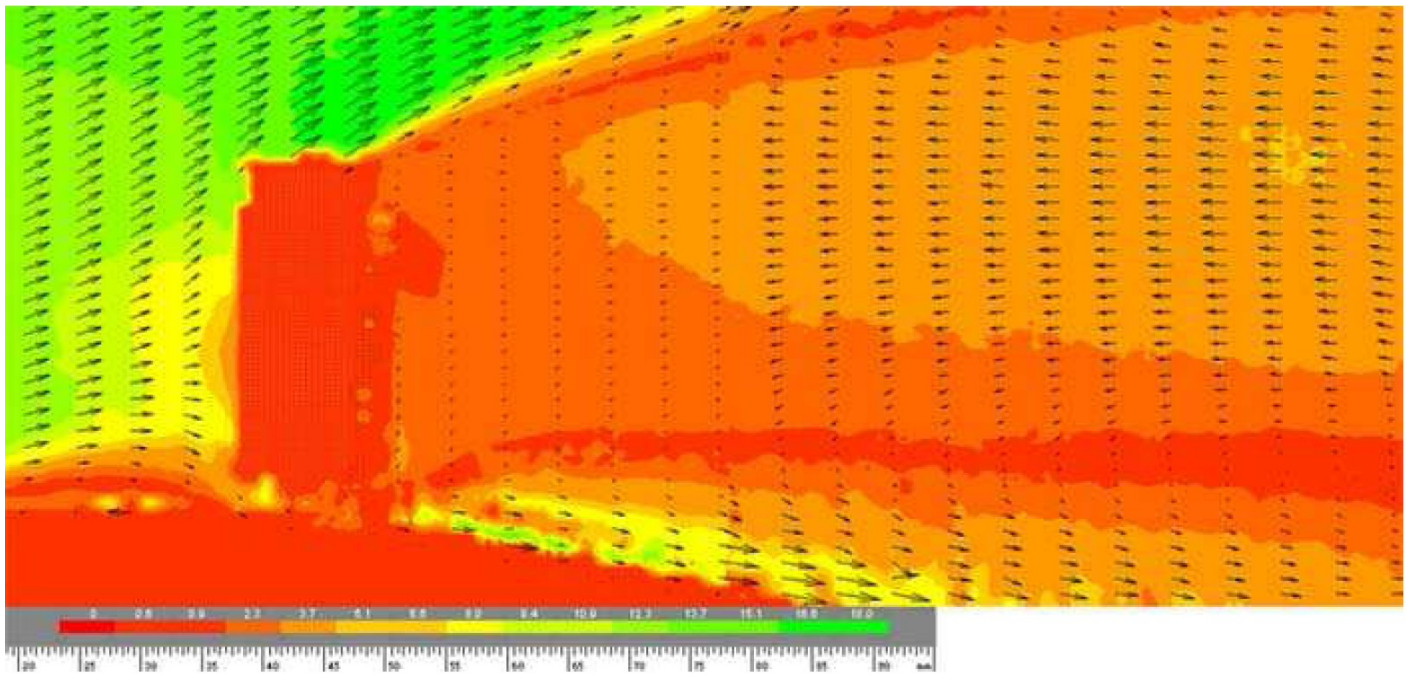


**Figure 7** Velocity distribution on FX66-17AII-182 airfoil with dive brake from PIV measurement, the velocities range: 0 – 18.5 m/s.

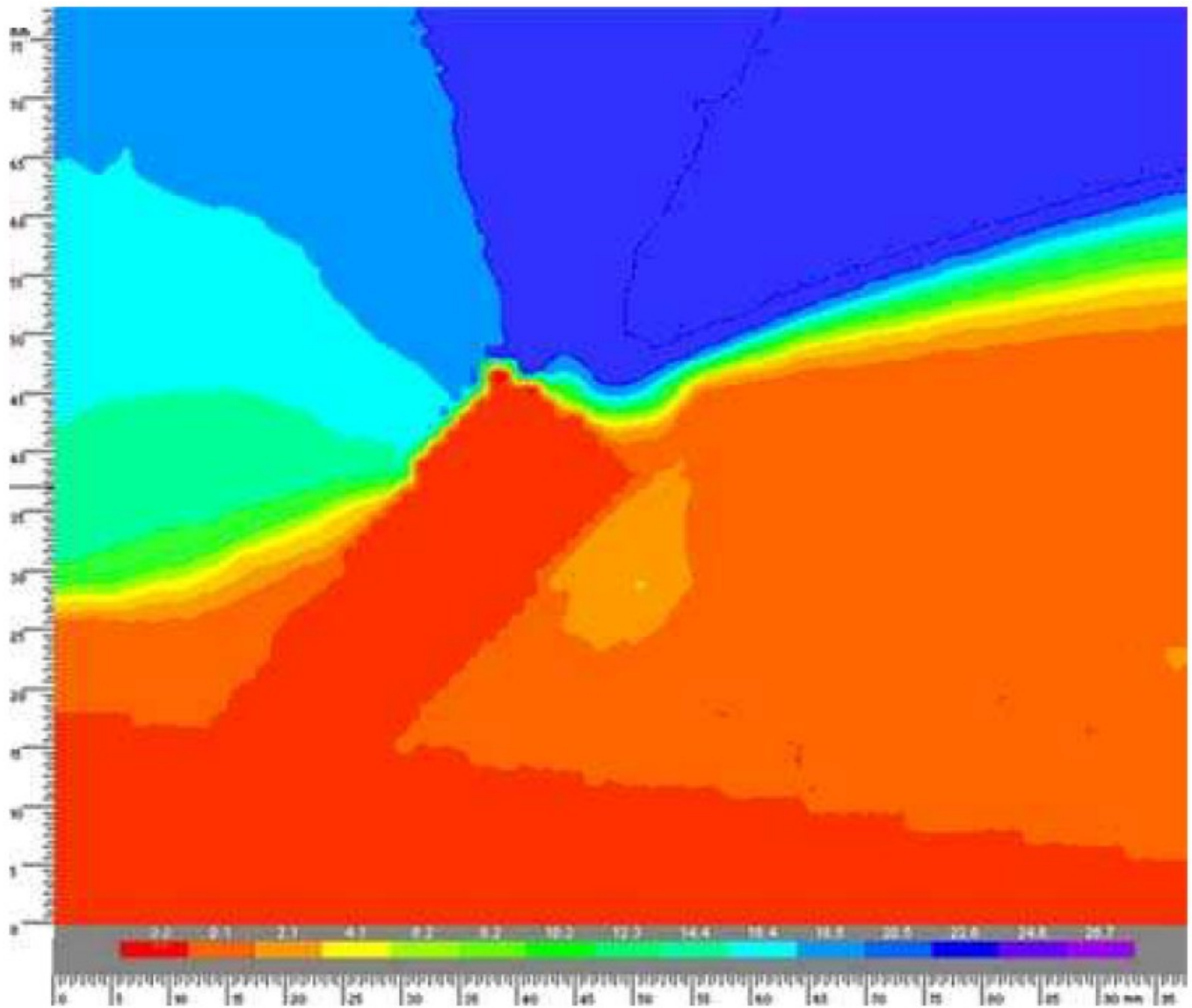


**Figure 8** Velocity distribution on NACA 23012 airfoil with spoiler flap from PIV measurement, the velocities range: 0 – 26.7 m/s.

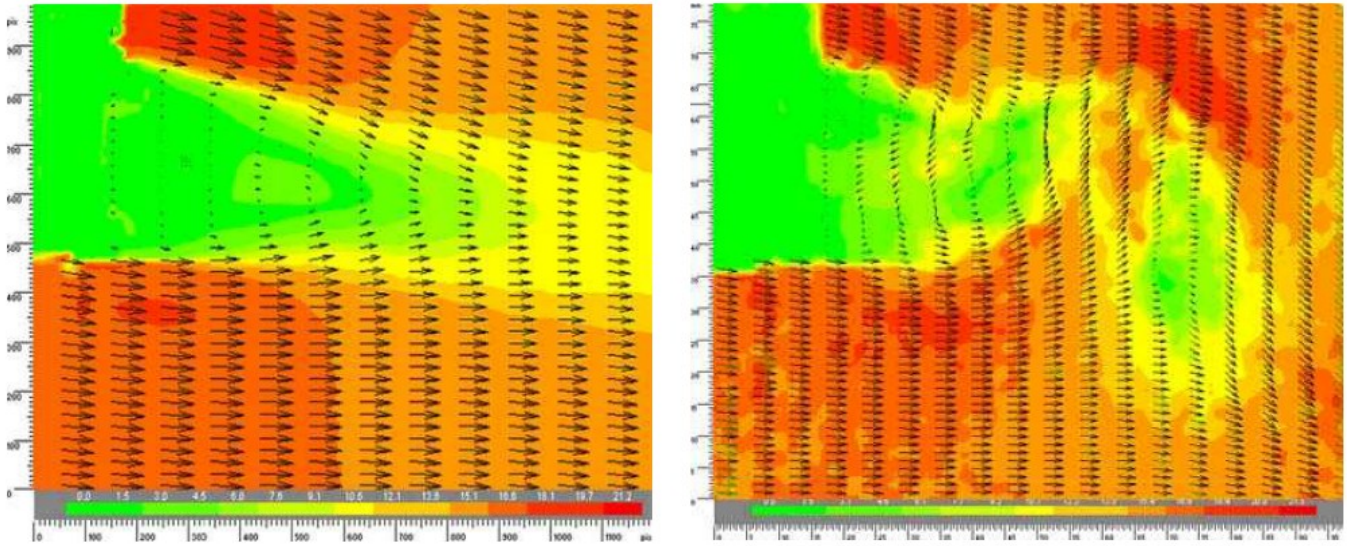


**Figure 9** Velocity distribution on MS 03-313 airfoil with split flap. Left image – time averaged flow, right image – instantaneous image of flow. PIV measurement, the velocities range: 0 – 21.5 m/s.

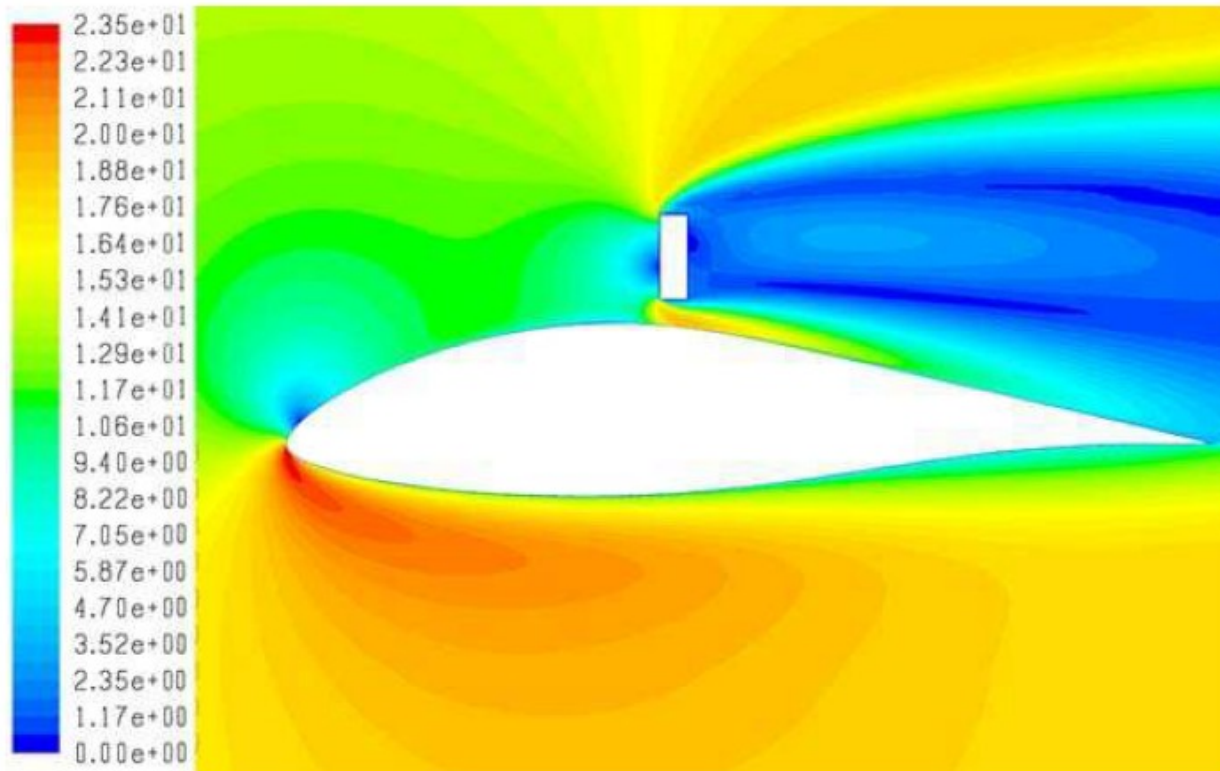


**Figure 10** Velocity distribution from numerical analysis [m/s] around FX66-17AII-182 airfoil with dive brake extended.

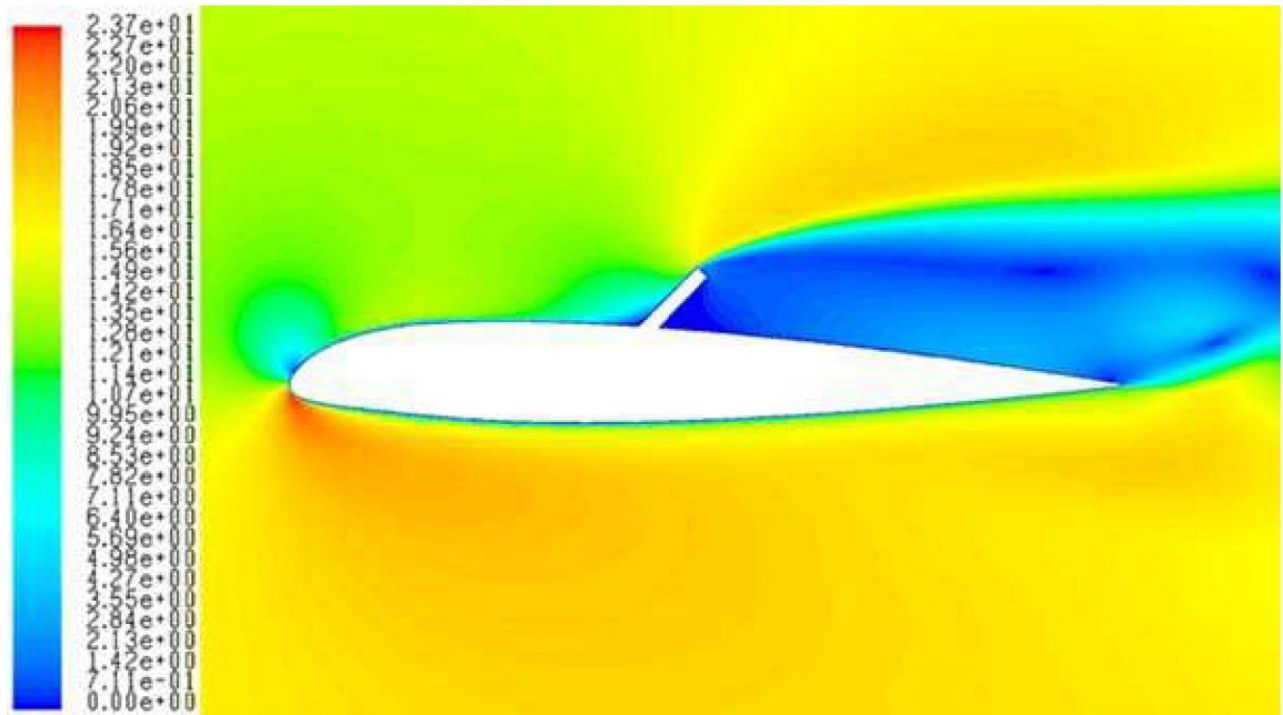


**Figure 11** Velocity distribution from numerical analysis [m/s] around whole NACA 23012 airfoil with spoiler deployed.

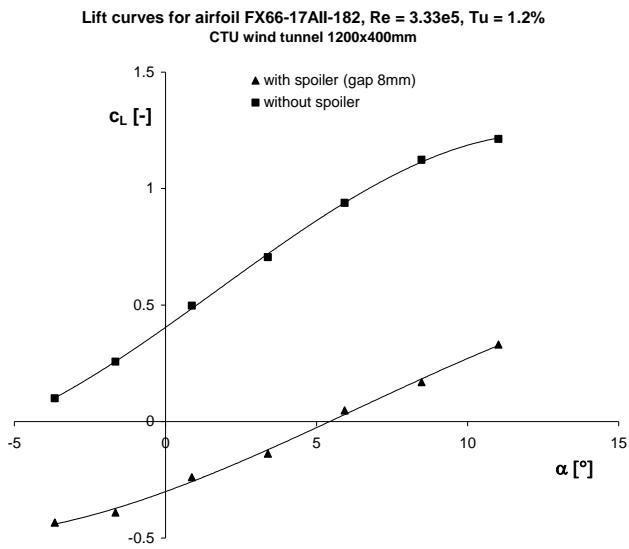


**Figure 12** Lift-curve slopes comparison of FX66-17AII-182 airfoil with and without spoiler extended.

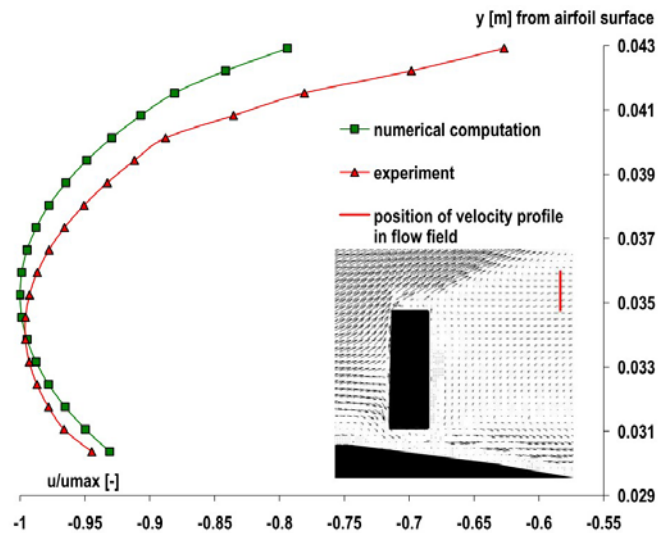


**Figure 13** Standard velocity profiles comparison of FX66-17AII-182 airfoil with dive brake extended.

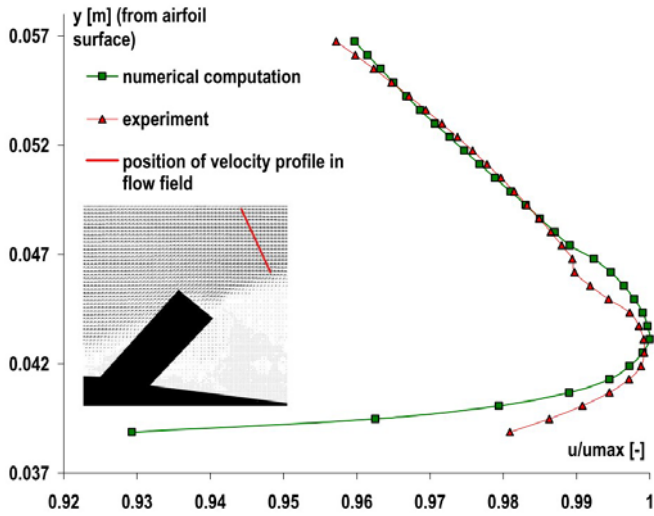


**Figure 14** Standard velocity profiles comparison of NACA23012 airfoil with spoiler deployed.

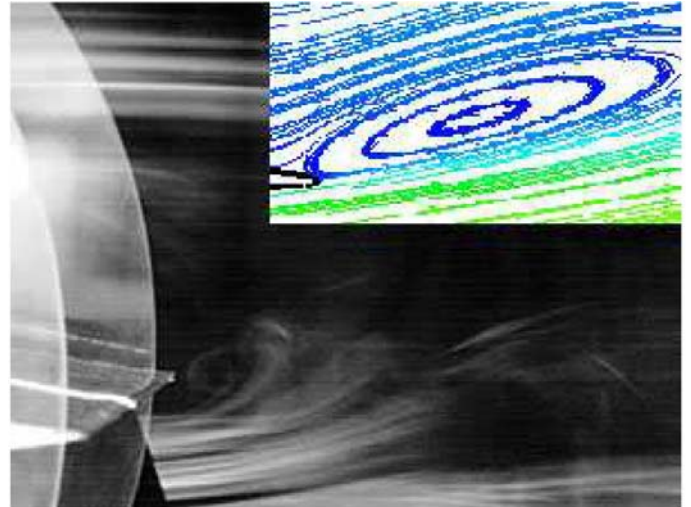


**Figure 16** Verification of vortex on trailing edge of NACA 23012 airfoil using smoke-wire visualization (picture in upper right corner: numerical analysis).

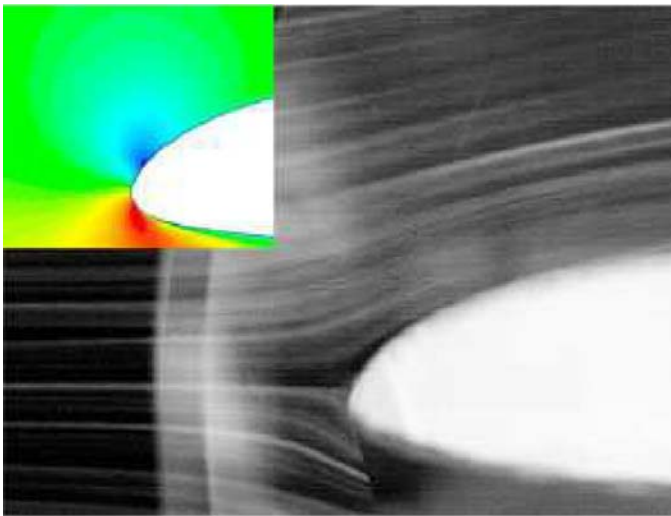


**Figure 15** Verification of stagnation point on leading edge of NACA 23012 airfoil using smoke-wire visualization (picture in left upper corner: numerical analysis).